

On the Parasitic Heat Transfer Between Dwellings in the Case of Individual Heating: First Results by Simulation Across the EU

Viola Iaria – Tor Vergata University of Rome, Italy – viola.iaria@uniroma2.it

Carlo Mazzenga – Tor Vergata University of Rome, Italy – carlo.mazzenga@uniroma2.it

Vincenzo A. Spina – Sapienza University of Rome, Italy – vincenzo.spina@uniroma1.it

Abstract

In residential applications with individual thermostat controls, a major problem arises as a consequence of heat transfer between conterminous dwellings when at least one is unconditioned or under-conditioned. Any absence of people, or under-heating by any tenant, can significantly falsify the accounting of heat flows, particularly in the case of highly performing building envelopes. In this paper, the effects of this kind of “parasitic” heat transfer across the apartments of a residential building is simulated, using, as a preliminary approach, a simplified proprietary calculation code, which considers different set-points of thermostats assumed by different tenants, and internal gains as occupancy-related. Results show that there is a real need for thermal insulation of interior partitions and, especially for existing buildings, diseconomies as much high as the climate is mild. These results reveal the intrinsic heat accounting iniquity as a result of parasitic heat transfer through conterminous dwellings.

1. Introduction

In the wide parameter space involved in the correct assessment of the thermal performance of a building, the basic role played by the occupant’s behavior appears not to have yet been deeply explored. The European Directive 2012/27/EU on energy efficiency – the ‘EED’ (European Parliament, 2012) – suggests that individual heat metering in multi-apartment buildings is a remarkable driver of energy savings. Nevertheless, EU member States intend to implement the EED quite differently. Some countries, such as Germany or Austria, make very few exceptions to the commitment; while in other countries, such as France or Sweden, the duty appears less severely enforced. In countries like Italy, where resi-

dential multi-storey buildings have always been conceived as merely isothermal inside (Hensen and Lamberts, 2011; Shiel et al., 2018), with and interior partitions (interfloor slabs and walls) hence designed to be uninsulated, economical suitability (Celenza et al., 2016) of the EED appears conflicting. The advent of individual heat metering and accounting made – unexpectedly as well as inappropriately (Spina, 2017) - a huge amount of interior partitions highly heat dissipating, because it is unable to prevent heat exchanges (Pessenlehner and Mahdavi, 2003). On this matter, no relevant improvements were added by the recent European Directive 2018/844/EU (European Parliament, 2018), except for the use of Smart Readiness Indicators (SRI); by comparison, imbalances in room temperature levels were incautiously promoted.

2. Simulation

As an initial approach to examine this issue, a suitable SW code, already used (Spina et al., 2017) by some of the authors, was implemented to simulate the effects of different behaviors by tenants on energy consumption and metering.

2.1 The Source Code Structure

Weather data, set-point temperature levels, building envelope and fabric properties are described partly by deterministic, partly by stochastic models using algorithms and source code routines. In the present application one reference day per each month, hourly simulation time-steps, two selected typical surface exposures (NE and SW), together with a 13 h per day (7.00 am–20.00) heat metering

and accounting range at the coils, are assumed in iterative procedures.

2.1.1 The climatic model

The model is extensively described elsewhere (Spena et al., 2010). Solar radiation on the building envelope is simulated through the atmosphere model provided by Ashrae (ASHRAE, 2017). To explore to what extent the implementation of the EED can differ across the EU, two locations representing respectively a continental (Berlin, lat. 52.3°N) and a Mediterranean (Rome, lat. 41.5°N) climate condition of a nearly equal longitude (12.3° vs 13.2°) are compared. Cloudiness is also considered, by means of the Monte Carlo-based algorithm discussed in Spena et al. (1997). Thermal flows through walls are obtained from Fourier’s general equation, also taking into account the inward flowing fraction of absorbed solar radiation by means of the so-called sol-air temperature (ASHRAE, 2017). A generally stabilized periodic regime is simulated (Spena, 1984; Tabunschikov, 1993) as follows:

$$q(t) = U * (\overline{Tsa} - Ti) + U * \sigma * (Tsa(t - \varphi) - \overline{Tsa}) \quad (1)$$

where:

- t = time (hrs)
- U = overall heat transfer coefficient ($\frac{W}{m^2 \cdot K}$)
- Tsa = sol-air temperature (°C)
- Ti = indoor air temperature (°C)
- σ = heat flow damping (dimensionless)
- φ = phase-lag (hrs).

Heat flow damping and phase-lag are estimated according to the Alford, Ryan and Urban model (Alford, 1939). Corrective factors are introduced in (1) to properly consider the effects of solar radiation on walls. The sol-air temperature effect is neglected in the case of transparent components as it involves an increase in the overall heat gain of no more than 1%.

Outdoor weather data are taken from reference years described elsewhere (Spena, 2017; <http://www.eurometeo.com>); one representative day per month, namely the 15th of each month, is considered.

2.1.2 The building model

A dynamic simulation was carried out on the base portion of a residential multi-apartment building shown in Fig. 1, with a rectangular-prism geometry. Two exterior walls are assumed (black bold lines), one facing NE, the other SW. Interior walls (blue lines) are assumed (see § 2.2) as adiabatic. The total floor area (of about 160 m²) is divided equally between the two apartments. To evaluate internal gains from occupancy, a presence of 0.025 persons per square meter, with a simultaneity factor of 0.5 (Jian, 2018; Mahdavi, 2011) is assumed. The glazing area is assumed to be 15% of the exterior surface.

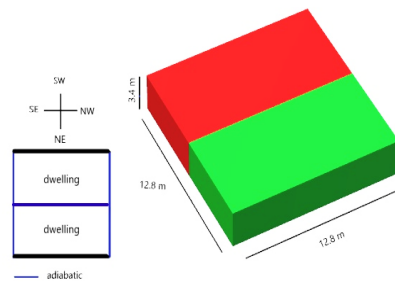


Fig. 1 – Sketch of the dwellings

Two levels of insulation of the envelope are considered: high (HI), and low (LI) insulation. U-values are as follows (Table 1):

Table 1 – Overall heat transfer coefficients for the envelope

Insulation	U_{wall} ($\frac{W}{m^2 \cdot K}$)	U_{window} ($\frac{W}{m^2 \cdot K}$)	U_{roof} ($\frac{W}{m^2 \cdot K}$)
HI	0.30	1.51	0.28
LI	0.93	4.07	0.81

Correspondingly, two values of the global solar heat gain coefficient SHGC are considered: 0.150 (HI) and 0.187 (LI). Values also include shading and framing effects.

2.1.3 The facilities model

Because of the capabilities of the model, the following assumptions are made. A centralized (or district) hot water system feeds room heating coils. According to the EED, individual heat metering and accounting by means of cost allocators is shared by all tenants. In accordance with the Italian UNI 10339 standard, an average continuous infiltration rate of 0.25 ACR (air change rates, i.e. volumes per hours)

is supposed. This is consistent with the above occupancy simultaneity factor of 0.5. As far as visual comfort for occupants is concerned, lighting conditions refer (CEN, 2017) to standard EN 15193-1. Daylighting and/or artificial lighting always ensure an average level of 125 lx. Over time, the contribution of daylighting is evaluated through the mean daylight factor FDL as follows:

$$FDLm = \frac{\sum_i \tau_i * S_i * \psi_i * \varepsilon_i}{(1 - rm) * Stot} \quad (2)$$

where:

- i = ith glazing surface
- τ = glazing solar transmittance
- S = glazing area
- ψ = rear positioning factor (with respect to the facade)
- ε = shape factor
- rm = glazing mean light reflectivity
- $Stot$ = overall room interior surface.

For each room space, FDLm is the ratio between the interior and exterior illuminance, measured on a horizontal plane viewing the entire sky in overcast conditions (the amount of available light is therefore independent of exposure). Once daylighting levels, standard requirements (Fontoynt, 1999; Hunt, 1979), and lighting efficiency (we suppose the use of fluorescent lamps with 50 lm/W) are given, the FDL factor enables us to estimate hourly the internal gains resulting from complementary artificial lighting.

2.2 The Cases Studied

The simulation was applied to the described base portion of the building, considering different situations. The period of year studied was the winter season, from November to March, when the most severe weather conditions are experienced by both locations. Energy balances take into account the two opposite building facades (NE and SW); hence, in addition to heat flows through walls and windows, differences in heat demand are due to solar radiation-related loads. Internal gains result from artificial lighting – which is zeroed in the case of unoccupied dwellings – and from occupancy of the dwelling.

To start with, the most significant case of parasitic heat flow – that which occurs through interfloor slabs, rather than through vertical partitions – will be considered.

heat flow through interfloor slabs also took into account a realistic air temperature stratification: a gap of + 0.5 °C and of – 0.5 °C from the mean dwelling temperatures was assumed in the ceiling and on the floor of each room respectively. Moreover, slightly different values of the combined (radiative plus convective) interior surface coefficients were used, according to the different free convective motions (Fisher and Pedersen, 1997; Tabunschikov, 1993), leading to the following U-values for the horizontal walls: $U_{downward} = 1.58 \frac{W}{m^2 * ^\circ C}$; $U_{upwards} = 1.51 \frac{W}{m^2 * ^\circ C}$.

The thermal inertia of the walls was not considered for the interfloor slabs, for the following reasons:

- i) their thermal mass together with surface temperature oscillations are one order of magnitude lower than those on the external walls; ii) there is no solar radiation contribution (which might increase imbalances).

The calculations in relation to heating demand (namely, of thermal energy end-uses demand) were made regardless of the type of heating or HVAC equipment.

2.2.1 Basic heat demand

A preliminary study (base cases) was carried out to determine the basic heating demand with all apartments occupied and kept at the same standard temperature (20 °C). Four cases were obtained by combining the two different envelopes of Table 1 with the two EU locations, namely Berlin and Rome. Following this, the simulated cases of unbalance were as follows.

2.2.2 Apartment occupied, kept at a lower temperature

The apartment above the reference apartment (20 °C) is kept, by the tenant, at a temperature from 1 to 5 °C (namely at set points from 15 to 19 °C) lower.

2.2.3 Apartments left unoccupied, heating turned off

This scenario contains two relevant sub-cases:

1. an unoccupied apartment between two apartments kept each at a standard temperature
2. an occupied apartment kept at a standard temperature, placed in between two unoccupied apartments, with the upper apartment being on

the top floor, and the lower apartment on the ground floor.

All other conditions being equal, infiltration thermal loads will depend on both outdoor and indoor temperatures. It was also assumed that in the case of overheating (an excess in heat gains), no cooling is provided, with the exception of free cooling by opening the windows.

3. Results

3.1 The Cases of Balanced Dwellings: Basic Heat Demand

With a standard average indoor temperature of 20 °C for all apartments, and under steady interior conditions, only small thermal flows occur, as a consequence of stratification, from bottom to top. Apart from border apartments such as those on the top-floor or ground-floor (IEA, 2014), the vertical thermal balance is zeroed for each intermediate dwelling; its hourly heating demand is merely given by the algebraic sum of exterior surface-related thermal loads.

As an example, Fig. 2 shows the hourly energy loads of a December reference day of one of the apartments facing NE. The case is that of a low-insulated building located in Rome. In Fig. 2 the hourly trend of heat flow through windows is specular to the one of outdoor temperature while the trend of the heat flow through the walls is damped and time-shifted by their thermal mass. At the considered exposure, solar gains occur in the first part of the day, while artificial lighting occurs in the early morning and in the evening.

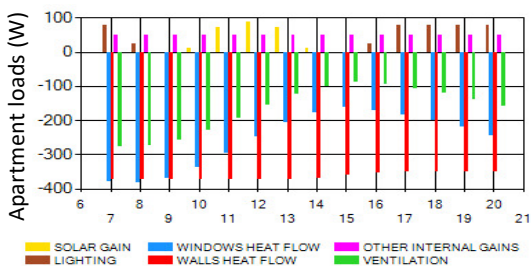


Fig. 2 – Rome, December, LI case, NE exposure. Energy demand over the reference day

As an insight into the effects of orientation, Fig. 3 reports the different percentages of total heating de-

mand – for the coldest month and the winter season overall – corresponding to the different exposures. In the considered reference year, the coldest month for Berlin and Rome is respectively January, and December. As expected (Brouns et al., 2016), apartments facing NE always require more heat than those facing SW because of the lower total (direct plus diffuse) solar radiation; the more the solar radiation-related thermal loads increase, the more this gap widens (as for high insulation and high solar radiation, at a given percentage of fenestration).

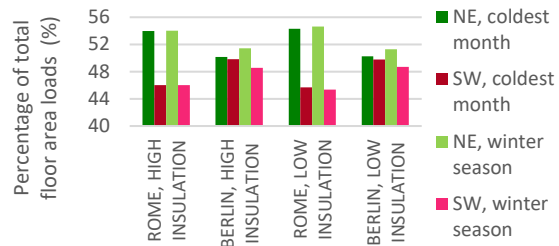


Fig. 3 – Percentages of total heating demand



Fig. 4 – Berlin, March, HI case. Energy demand over the reference day

As a matter of interest, Fig. 4 shows, for the northern location (Berlin), overheating (solar and other gains exceeding heat dissipation through walls and windows) of SW side-spaces around midday. Even though with different intensities, simulations show that, from a qualitative point of view, this phenomenon recurs often throughout the whole winter season.

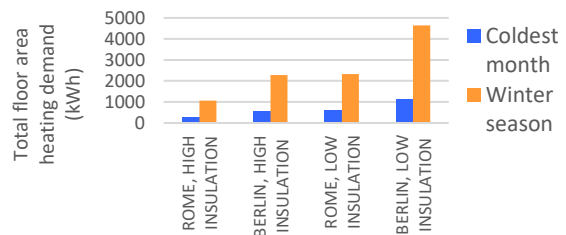


Fig. 5 – Dwellings overall basic heating demand

Finally, in Fig. 5 the overall basic heat demands of the dwellings are reported. As expected (Pedrini et al., 2002), they increase in case of low outdoor temperatures (i.e. at higher latitudes) and of poor building envelope insulation.

3.2 The Case of Unbalanced Dwellings

3.2.1 Upper apartment at a lower temperature

In this example, the upper apartment temperature is kept from 1 °C to 5 °C below the standard level (see Fig. 6). From this point onwards, green graphs will refer to NE exposure, and red graphs to SW exposure.

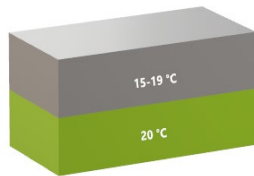


Fig. 6 – Two-apartments case sketch

Since now on, as an indicator of the relevance of the problem posed by the present paper, the ratio R between the “parasitic” heat loss to other neighboring apartments, and the basic heat demand of a considered apartment kept at a standard temperature, will be adopted. The results are summarized in Figs 7 and 8 as a function of the temperature gap (°C) which is the driving cause of the effect.

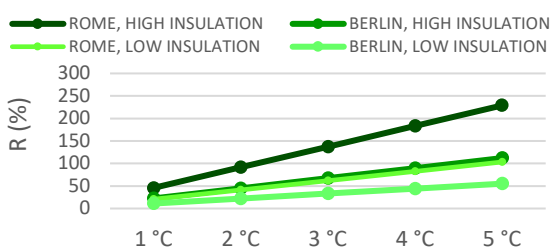


Fig. 7 – NE exposure. Relative increase on heating demand

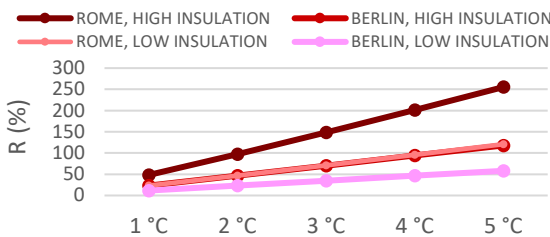


Fig.8 – SW exposure. Relative increase on heating demand

At any temperature difference, all apartments facing SW show relative parasitic increases in heating demand R that are slightly higher than for NE facing apartments, according to their lower overall basic heating need. More specifically, at the given conditions, whatever the climate, a temperature difference of 2 °C in case of high insulation has the same effect as a temperature difference of 4 °C with low insulation; inversely, with an equal temperature difference, departures are halved. It is clear that relevant parasitic heat transfer occurs (with R values up to a factor 2.5) not only in Northern climates (such as Berlin) with high insulation, but also in Southern climates (such as Rome) with low insulation, particularly in apartments with SW exposures. On the other hand, with high latitudes (such as Berlin) and weak insulation, parasitic heat flow across interfloor slabs remains lower than heat flow towards the outside, at least until the temperature difference between the apartments remains below 4÷4.5 °C.

3.2.2 Unoccupied border-lying apartments

In this scenario, two main situations are considered: Case 1, shown in Fig. 9, is an unoccupied apartment lying between two occupied apartments both kept at a standard temperature (20 °C); and Case 2, shown in Fig. 10, is an occupied apartment kept at a standard temperature, located between two unoccupied apartments, the upper apartment being on the top floor, and the lower apartment on the ground floor. For each situation, both NE and SW exposures were studied.

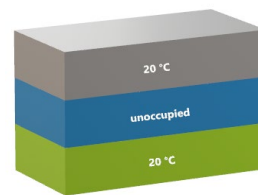


Fig. 9 – Unoccupied border-lying apartments. Case 1

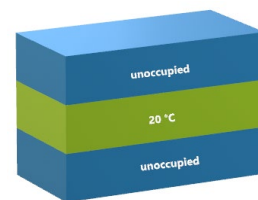


Fig. 10 – Unoccupied border-lying apartments. Case 2

It was assumed that in the unoccupied apartments all the coils were switched-off. Thus, in both cases, in the unoccupied apartment the lower the insulation and the lower the outdoor temperatures, the greater the decrease in the indoor average temperature. The results of the simulations indicated that low insulation leads to average temperatures in the unoccupied apartments as follows:

- from a minimum of 10.6 °C (Case 2, in January) to a maximum of 17.8 °C (Case 1, in March) for the Northern (Berlin) location
- from a minimum of 14.0 °C (Case 2, in December) to a maximum of 18.9 °C (Case 1, in March) for the Southern (Rome) location.

Correspondingly, high insulation led to average temperatures of the unoccupied apartments as follows:

- from a minimum of 15.6 °C (Case 2, in January) to a maximum of 19.1 °C (Case 1, in March) for the Northern (Berlin) location
- from a minimum of 16.3 °C (Case 2, in December) to a maximum of 19.6 °C (Case 1, in March) for the Southern (Rome) location.

It may be observed that with high insulation, the coldest space is always the ground floor; by comparison, with low insulation the coldest space is always the top floor. In Figs. 11 and 12, the relative parasitic increase in heating demand R through the interfloor slabs for the apartment occupied and kept at 20 °C is reported, for both the considered exposures.



Fig. 11- NE exposure. Relative increase on heating demand



Fig. 12 - SW exposure. Relative increase on heating demand

These results appear qualitatively similar to those previously obtained: the greatest seasonal relative increase in R always corresponds to Case 2, while the apartment facing SW remains more sensitive to the parasitic effect. More importantly, the effects of parasitic heat flows in Mediterranean climates (such as Rome) appear to be greater, even with low insulation (and particularly with SW exposures), than in continental climates (such as Berlin), even with high insulation. The difference between R values for Case 2 and Case 1, while decreasing as both insulation and climate warmth diminish, remains high, ranging from a factor of 5 (low insulation) to 8 (high insulation).

4. Discussion

Figs. 13–16 summarize and compare the results in terms of homogeneous configurations in order to better understand what has been discussed and presented thus far.

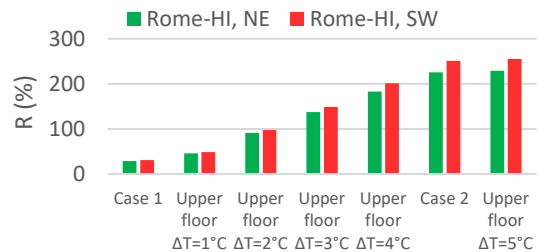


Fig. 13 – Rome-HI. Comparison of the results

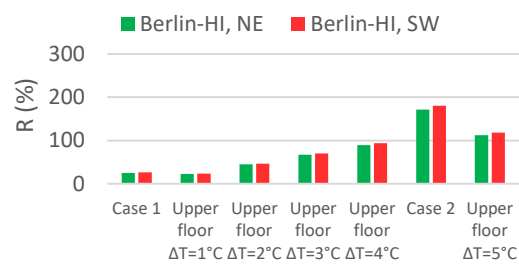


Fig. 14 – Berlin-HI. Comparison of the results

As previously observed, the NE facing apartments present values of R that are again slightly lower than for the SW facing apartments. This is due to the fact that the parasitic additional heat flow - being equal for both exposures - has a greater impact when basic heat demand is lower (solar and other gains are zeroed for unoccupied apartments in this con-

figuration). For both locations, greater R values are shown with high envelope insulation and with SW exposure.

For Rome, low external envelope overall heat transfer coefficients cause greater R values for an apartment kept at 20 °C and lying in contact with an unoccupied apartment (for the whole winter season), whilst high external overall heat transfer coefficients tend to reduce the drops in temperature in the unoccupied apartments. In the latter case, the worst scenario is that in which the upper apartment is constantly kept at the minimum considered temperature (15 °C).

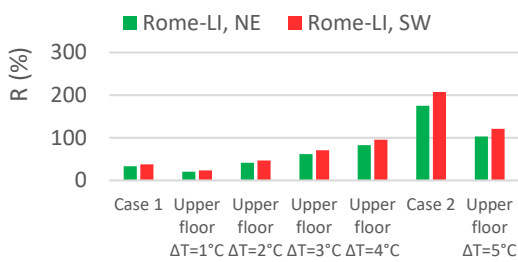


Fig. 15 – Rome-LI. Comparison of the results

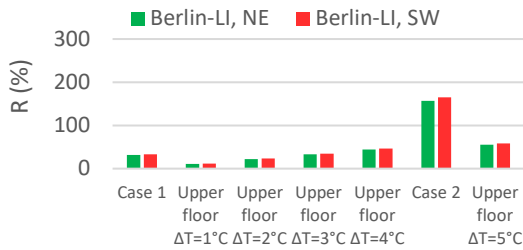


Fig. 16 – Berlin-LI. Comparison of the results

For Berlin, given that weather conditions are generally more severe, Case 2 is always the worst, regardless of the insulation level of the building envelope. The order of criticality is almost the same for the case of an apartment in Rome with low insulation and an apartment in Berlin with high insulation; in mild climates a lower level of building envelope insulation has the same effect as a higher envelope insulation level in severe climates.

As far as uncertainties are concerned, it's worth to remember that any limitation in the level of details allowed by a model, as well as any simplifying assumption made in the calculations, unavoidably can affect the results. As an example, this is the case of having neglected heat flow through vertical partitions, or of having selected a specific accounting

time. Nevertheless, and especially in terms of comparisons, the importance of the problem identified in this paper remains clear.

5. Conclusions and Further Insights

The study has highlighted how individual heating in an existing multi-storey residential building, especially in mild climates, can lead to an involuntary (as well as unavoidable) increase in individual cumulated heat consumption up to a factor of 3 or 4 over its basic voluntary heat demand.

Owing to the complexity of the topic, the initial results reported in this paper were obtained by using a set of simplified assumptions, and thus require further investigation. Nevertheless, from a qualitative point of view, the results clearly show that the differing use of individual heat metering and accounting for the buildings considered implies: i) a self-evident heat accounting iniquity in terms of parasitic heat transfer between conterminous dwellings; ii) a strong need for thermal insulation of interior partitions (especially of interfloor slabs), which is even more urgent than that for exterior walls; iii) the necessity to explore any potential for mitigation of the problem by means of advanced domotics; iv) the need for more detailed audits and sensitivity analyses, particularly for Mediterranean weather conditions; v) the need for further research on tailored calibrations and accuracy evaluations, in addition to improved predictions and modelling of the behavior of occupants.

In any case, not only do improvements in regulatory frameworks appear necessary, but also changes in the design criteria for new buildings. In the meantime, the need for retrofits of existing buildings by means of interior partition insulation and – most of all – for urgent mitigations in heat accounting rules, appears to be self-evident.

References

Alford, J. S., J. E. Ryan, P. O. Urban. 1939. "Effect of heat storage and variation in outdoor temperature and solar intensity on heat transfer through walls." *Ashve Transaction* 45, 369.

- ANSI/ASHRAE. 2017. *Standard 140-2017, Standard Method of Test for the Evaluation of Building Energy Analysis Computer Programs*. American Society of Heating, Refrigerating and Air-Conditioning Engineers, Atlanta, GA.
- ASHRAE. 2017. *ASHRAE Handbook of Fundamentals*. ASHRAE. Atlanta (U.S.A).
- Brouns, J., A. Nassiopoulos, F. Bourquin, K. Limam. 2016. "Dynamic building performance assessment using calibrated simulation." *Energy and Buildings* 122: 160-174.
- Celenza, L., M. Dell'Isola, G. Ficco, M. Greco, M. Grimaldi. 2016. "Economical and technical feasibility of metering and sub-metering systems for heat accounting." *International Journal of Energy Economics and Policy* 6(3): 581-587.
- CEN - European Committee for Standardization 2017. *Energy performance of buildings - Energy requirements for lighting - Part 2: Explanation and justification of EN 15193-1, Module M9*. (UNI CEN/TR 15193-2:2017).
- Eurometeo website (<http://www.eurometeo.com>).
- European Parliament. 2018. *Directive 2018/844/EU*.
- European Parliament. 2012. *Directive 2012/27/EU*.
- Fisher, D. E., C. O. Pedersen. 1997. "Convective Heat Transfer in Building Energy and Thermal Load Calculation." *ASHRAE Transactions* 103(2): 137-148.
- Fontoyont, M. (edited by). 1999. *Daylight Performance of Buildings*. Routledge. London, U.K.
- Hensen, J.L.M., R. Lamberts (edited by). 2011. *Building Performance Simulation for Design and Operation*. Routledge. London, U.K.
- Hunt, D. 1979. "The use of artificial lighting in relation to daylight levels and occupancy." *Building and Environment* 14: 21-33.
- IEA - International Energy Agency. 2014. *Building Energy Simulation Test and Diagnostic Method (IEA BESTEST)*. *In-Depth Diagnostic Cases for Ground Coupled Heat Transfer Related to Slab-on-Grade Construction*. Approved by ASHRAE as an Addendum to Standard 140-2011.
- Italian Thermotechnical Committee (CTI). 1994. *UNI 10339 - Impianti aeraulici a fini di benessere. Generalità, classificazione e requisiti. Regole per la richiesta d'offerta, l'offerta, l'ordine e la fornitura*.
- Jian, Y. 2018. "Modelling and simulating occupant behaviour on air conditioning in residential buildings." *Energy and Buildings* 175: 1-10.
- Mahdavi, A. 2011. *People in Building Performance Simulation*. In Hensen, J.L.M., Lamberts R. *Building Performance Simulation for Design and Operation*. Routledge. London, U.K.
- Pedrini, A., F. S. Westphal, R. Lamberts. 2002. "A methodology for building energy modeling and calibration in warm climates." *Building and Environment* 37(8-9): 903-912.
- Pessenlehner, W., A. Mahdavi. 2003. "Building morphology, transparency, and energy performance." *Eighth International IBPSA Conference*. Eindhoven, the Netherlands, August 11th - 14th 2003.
- Shiel, P., S. Tarantino, M. Fischer. 2018. "Parametric analysis of design stage building energy performance simulation models." *Energy and Buildings* 172: 78-93.
- Spena, A. 1984. "Studio comparativo, mediante simulazione, della produzione combinata di energia elettrica, calore e freddo per la copertura dei fabbisogni di un comprensorio edilizio per attività terziarie." *Proceeding of XXXII ATI National Congress*. L'Aquila, Italy.
- Spena, A., A. Vitaliti, F. Cardarelli. 1997. "Primi risultati di un metodo per la generazione di congruenti valori orari della componente della radiazione solare al suolo." *Proceeding of LII ATI National Congress*, Cernobbio, Italy.
- Spena, A., C. Strati, G. D'Angiolini. 2010. "First Correlations for a Mediterranean Cloud Cover Model." *Proceeding of SPIE Solar Energy Plus Technology*. San Diego, U.S.A.
- Spena, A. 2017. "Efficienza energetica. Governare la complessità delle opzioni più avanzate." *La Termotecnica*, 11.
- Spena, A., V. Iaria, C. Mazzenga. 2017. "Dynamic Simulation of the Influence of Fenestration on Buildings Energy Consumption. A Comparison Between Northern and Southern Europe." *Proceedings of BSA 2017: Building Simulation Applications Conference*. Bolzano, Italy, February 8th - 10th 2017.
- Tabunshchikov, Y.A. 1993. *Mathematical Models of Thermal Conditions in Buildings*. CRC Press. Boca Raton, U.S.A.